[1.]Dragiša VILOTIĆ, [2.]Milija KRAIŠNIK, [3.]Mladomir MILUTINOVIĆ, [4.]Dejan MOVRIN, [5.]Marko VILOTIĆ, [6.]Jelica ANIĆ, [7.]Mirko FICKO

MATERIAL FORMABILITY AT BULK METAL FORMING, CRITERIA, METHOD OF DETERMINATION AND APPLICATION

[1,3-5.]University of Novi Sad, Faculty of Technical Sciences, Novi Sad, SERBIA
[2,6.]University of East Sarajevo, Faculty of Mechanical Engineering, BOSNIA & HERZEGOVINA
[7.]University of Maribor, Faculty of Mechanical Engineering, SLOVENIA

Abstract: Material formability it is material ability to deform permanently in different stress condition without structure damage. The fracture limit of material in bulk metal forming is based on fracture and formability criteria. In metal forming, two formability criteria and two workability diagrams are being used: a) the strain based and b) stress based formability diagram. Strain based formability diagram represents the dependence of the principal strains on the free surface of specimen at the moment of the fracture occurrence. The stress based formability diagram represents the relation between limit strain and stress triaxiality ratio in the zone of fracture. In this paper, methodology of formability diagrams determination is presented and application of formability diagram for the limit strain prediction in multi-stage upsetting of prismatic specimen by V-shape dies is performed.
Keywords: Material formability, Triaxiality stress ratio, Multy stage upsetting

INTRODUCTION

Material formability (or material workability) is material ability to deform permanently in different stress condition without structure damage. It is convenient to distinguish two groups of formability criteria, theoretical and empirical. Empirical criteria are based on experimental investigation of real forming processes and they can be presented by two variants of the formability diagram (FLD): a) the strain-based and b) the stress-based formability limit diagram.

Formability diagram based on strain criterion represents relationship between two principal strains in the moment of fracture appearance [5-14, 16-19]. Usually this diagram is used in conjuction with upsetting test with different initial geometry. The strain based formability diagram and, therefore, the corresponding fracture criterion are path-independent [19].

According to the stress criteria, limit strain mainly depends on the stress state in the critical zone of the specimen, i.e., in the zone of material damage. Generally, the material formability depends on two groups of factors:

- # type of material, and
- # process conditions.

Quantitative measure of formability limit is effective strain, (φ_e^l), i.e., strain at the moment of material structure damage, strain localization or can be defined by any other criteria. For the given material, with the defined initial microstructure and in cold forming conditions by quasistatic deformation, material formability is a function of stress state only [5]:

$$\varphi_e^l = F(T_\sigma) = F(\beta) \tag{1}$$

where: T_σ – stress tensor

β – triaxiality stress ratio at the critical point of specimen, i.e., at the point of structure damage. Stress indicator is defined as:

$$\beta = \frac{\sigma_x + \sigma_y + \sigma_z}{\sigma_e} = \frac{\sigma_1 + \sigma_2 + \sigma_3}{\sigma_e} \tag{2}$$

where: σ_e – effective stress.

σ_x, σ_y, σ_z– normal stress components in three orthogonal directions (x, y, z)

Graphical interpretation of the relationship (1) is the stress-based formability limit diagram [5]. This diagram shows that in bulk metal forming processes in which compressive stresses prevail ($\beta < 0$), values of limit strains achieved are higher than in the processes in which tensile stresses are predominant ($\beta > 0$).

Values of stresses in expression (2) are determined from the stress-strain relation and the Misses yield criterion.

In the upsetting process (Figure 1) crack occurs at the free surface of the cylinder and at that point plain stress state exists, because $\sigma_r = 0$.

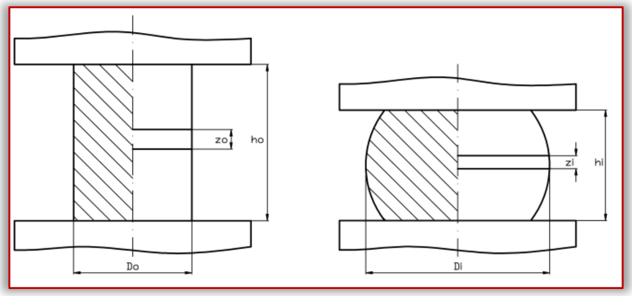

Figure 1. Upsetting of cylinder

Axial and tangential stress components could be determined by following expressions.

$$\sigma_z = \pm K[1 + \frac{(1+2\alpha)}{2+\alpha} + (\frac{1+2\alpha}{2+\alpha})^2]^{(-1/2)} \tag{3}$$

$$\sigma_\theta = \sigma_z \left(\frac{1+2\alpha}{2+\alpha}\right) \tag{4}$$

where α is the strains ratio:

$$\alpha = \frac{d\varphi_\theta}{d\varphi_z} \tag{5}$$

φ_θ and φ_z are logarithmic strain components in z and θ direction, experimentally determined by measuring specimen

$$\varphi_{\theta i} = \ln\left(\frac{d_i}{d_{i-1}}\right) \quad \varphi_{zi} = \ln\left(\frac{z_i}{z_{i-1}}\right) \tag{6}$$

It is also necessary to find relationship between these strain components. This function represents strain path in the area of crack appearance.

$$\varphi_\theta = B \cdot \varphi_z^2 + A \cdot \varphi_z \tag{7}$$

Stress factor β is determined by:

$$\beta = \frac{\sigma_r + \sigma_\theta + \sigma_z}{K} = \frac{\sigma_\theta + \sigma_z}{K} = \pm \frac{1 + \frac{1+2\alpha}{2+\alpha}}{\sqrt{1 + \frac{1+2\alpha}{2+\alpha} + \left(\frac{1+2\alpha}{2+\alpha}\right)^2}} \tag{8}$$

Stress-based formability limit diagram could be determined experimentally, by employing basic deformation models:

uni-axial tensile test, $\beta = +1$

torsion test, $\beta = 0$

uni-axial compression test, $\beta = -1$

At β=+1, the limit strain is experimentally determined by tension test at the stage of uniform deformation. It has also been shown that the uniaxial tension test can be replaced with the collar cylinder test for obtaining a point on the formability diagram where the fracture criterion based on an average value of the triaxiality ratio is adopted [12]. It is also shown that the collar test provides a more accurate prediction of the strain to fracture.

A more detailed determination of the formability limit diagram demands application of more sophisticated methods.

In the case of non-monotonous processes, stress indicator (β) changes during deformation and its mean value is inserted in the FLD diagram. The mean value of stress indicator is defined as [6,7,10,11]:

$$\beta_{av} = \frac{1}{\varphi_e^l} \int_0^{\varphi_e^l} \beta(\varphi_e) \cdot d\varphi_e \tag{9}$$

where: $\beta(\varphi_e)$ – history of triaxiality stress ratio which indicates change of stress-state as a function of effective strain.

It has been shown in [17] that the average value of the triaxiality ratio is expressed through the in-surface principal strains φl_1 and φ_2^l as:

$$\beta_{av} = \frac{2}{\varphi_e^l}\left(\varphi_1^l + \varphi_2^l\right) \tag{10}$$

In this paper the experimental methodology for determination of formability limit diagrams (strain-based and stress-based) in bulk metal forming is presented. The material used in the experiments was steel C45E (Č.1531).

EXPERIMENTAL DETERMINATION OF FORMABILITY DIAGRAMS

The remaining part of this work shows the results of experimental determination of formability diagrams for two variants. The diagram was determined based on the results of basic tests: RT – Rastegaev test (cylinder upsetting without friction influence), BC – cylinder upsetting, T – torsion test, CC – collar cylinder test [7,12,13]. Additional tests (Type 1–5) were performed by die upsetting of five types of non-axisymmetric specimens [18].

Table 1. Basic formability tests [7,12,13]

Test specimens		
Type of tests	Rastegev	Basic cylinder
Test specimens		
Type of tests	Collar cylinder	Torsion

Table 2. Additional formability tests [18]

		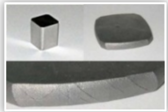
Type 1	Type 2	Type 3
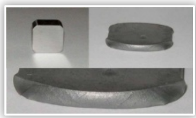		
Type 4	Type 5	

— Strain based formability limit diagram

Based on the strain path for the different experimental processes (standard and additional test, mentioned before) the strain based formability diagram is determined.

Strain path curves for different specimens are shown in Figure 2. The limit line was derived by approximation of final values for the strains (on the strain path curve) of particular tests – Figure 2.

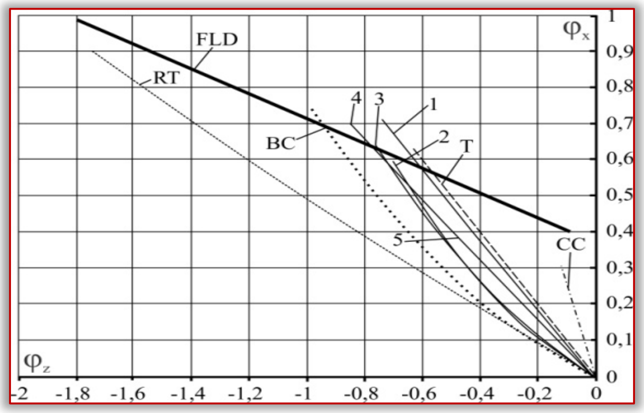

Figure 2. Strain-based formability diagram for steel C45E [18]
Basic tests: 1; RT–Rastegev test, BC–basic cylinder test, T–torsion test
CC–collar upsetting test, 1–5 additional tests [18]

— Stress-based formability limit diagram

The stress-based formability diagram (Figure 4) was generated applying the methodology described in the introductory section, based on the experimental data for the basic and additional forming methods. Essentially, the methodology used for constructing this diagram is based on the strain path diagram for the particular forming process shown in Figure 2, which allowed determination the history of triaxiality stress factor (β) using formula

(8). The history of triaxiality stress ratio for the standard and additional tests is presented in Figure 3.

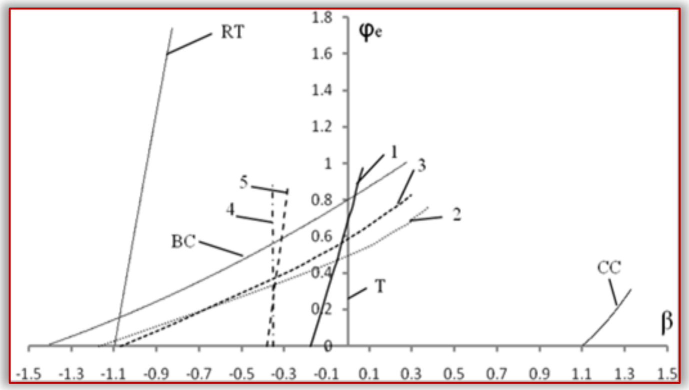

Figure 3. History of triaxiality stress ratio for different specimens: RT – Rastegaev test, BC – cylinder upsetting, T – torsion test, CC – collar cylinder test, 1–5 additional tests [18]

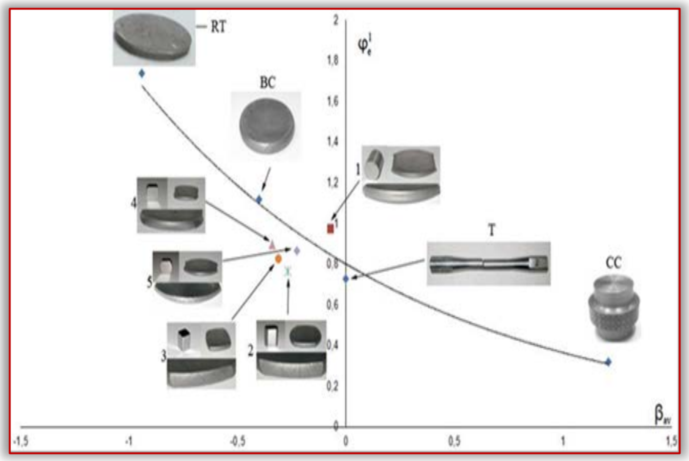

Figure 4. Stress-based formability limit diagram of steel C45E: RT–Rastegaev test, BC–cylinder upsetting, T–torsion test, CC–collar cylinder test, 1–5 additional tests [18]

Based on the history of triaxiality stress ratio and using formula (9), mean value of factor β_{av} was calculated.

Stress based formability diagram represents relationship between limit strain (φ_e^l) and average values of triaxiality stress ratio (β_{av}) – Figure 4.

APPLICATION OF FORMABILITY LIMIT DIAGRAM

In metal forming process forming limit diagram is used for fracture prediction, i.e. for the design and optimization of the number of forming phases. Same procedure may be used in metal structure load analysis. At first, it is necessary to create formability limit diagram for specified material and then to analyse the stress state and the triaxiality stress factor at sample bulk. For stress-strain state analysis in bulk specimen finite element method is recommended, i.e. application of proper software (SimufactForming, Abaqus, and Deform, etc.).

Presented below are the results of material formability analysis for multistage upsetting by V-shape dies of the prismatic billets made of Č.1221 [20]. The purpose of the analysis is to examine potential limit strain in this process, at upsetting with 17 stages, with sample rotation for 90° after each phase. Limit strain prediction is carried out by numerical analysis of upsetting by V shape dies of samples made of Č.1221. For this analysis, SimufactForming V10 software was used.

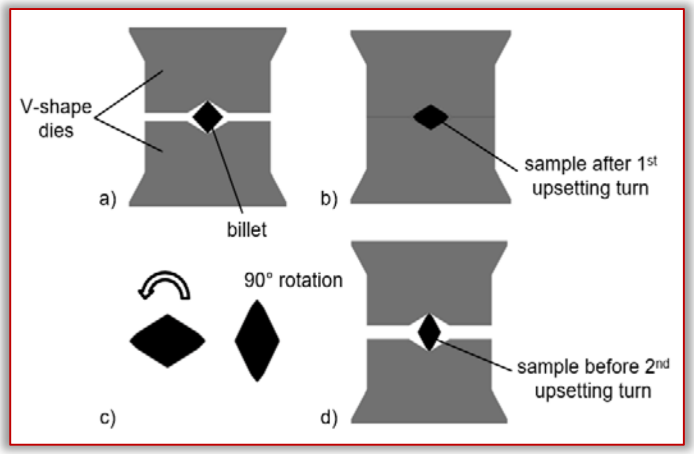

Figure 4. Multi stage upsetting of prismatic specimen by V-shape dies [20]

Table 3. Numerical simulation of multistage upsetting by V shape die [20]

No.	Effective strain	Effective stress
1	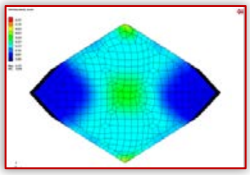	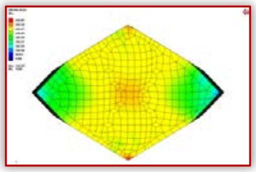
3	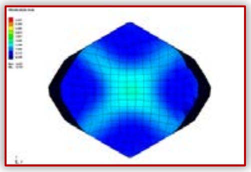	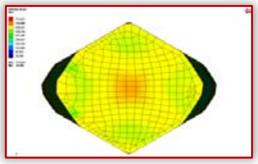
7	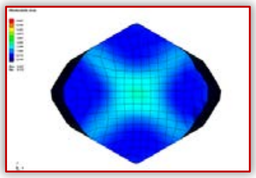	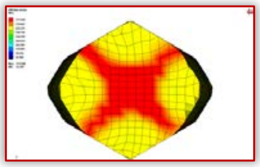
11	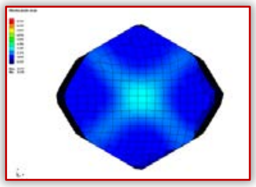	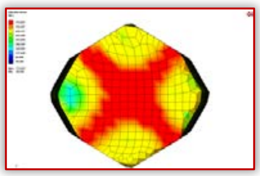
15	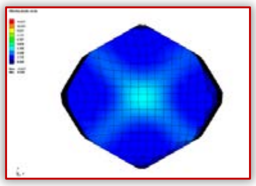	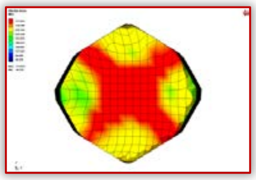
17	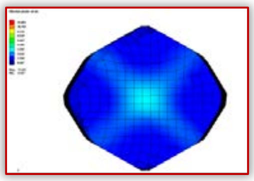	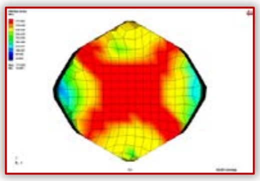

Triaxiality stress ratio analysis was carried out for the critical point on the specimen that is located at the centre of free (forehead) surface. The triaxiality stress factor is determined from the hydrostatic stress and the effective stress at the centre of the sample surface obtained by numerical simulations. The change of the triaxiality stress factor for different upsetting stages and corresponding effective strain values, at the centre of the sample forehead, is presented in table 4.

Table 4. Triaxialiti stress factor in correlation with effective strain

Upsetting stage	1	3	5	7	9
φ_e	0.39	1.58	2.29	2.61	2.83
β	- 2.88	- 2.38	- 1.95	- 1.95	- 1.91
Upsetting stage	11	13	15	17	
φ_e	2.98	3.14	3.28	3.34	
β	- 1.68	- 1.56	- 1.44	- 1.17	

FLD for Č.1221 (annealed) determined experimentally by the cylinder upsetting with flat plates, the torsion test and the tensile test [15]. Based on the data from Table 4, history of triaxiality stress ratio was identified and approximated by following equation:

$$\beta = 0{,}09 \cdot \varphi_e^2 + 0{,}156 \cdot \varphi_e - 2{,}925 \qquad (11)$$

Average value of triaxiality factor was determined by formula (9):

$$\beta_{av} = \frac{1}{3{,}34} \int_0^{3{,}34} (0{,}09 \cdot \varphi_e^2 + 0{,}156 \cdot \varphi_e - 2{,}925)\, d\varphi_e = -2{,}32 \qquad (12)$$

By using numerical analysis, average value of triaxiality factor β=–2,32 with corresponding value of limit strain $\varphi_e^l = 3{,}34$ was calculated. The illustration of fracture incidence at multistage upsetting of prismatic sample is presented at Figure 5.

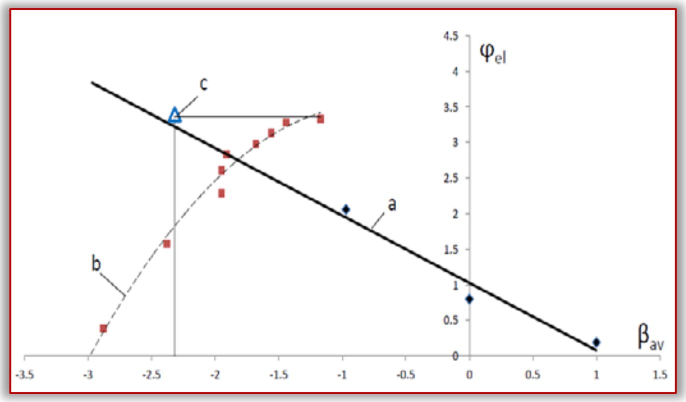

Figure 5. FLD for Č.1221 and the position of multi stage upsetting by V shape dies after 17 stages: a–FLD, b–history of β factor, c– estimated limit strain

DISCUSSION OF RESULTS AND CONCLUSION

- In the metal forming technology two formability criteria can be applied strain-based and stress-based criterion.
- Strain-based formability criterion is simple for application because it is based on strain determination in the material fracture zone. Due this feature, its application is limited to processes where fracture occurs on the free surface of workpiece.
- Stress-based formability criterion represents limit strain dependence from a stress state in the zone where material fracture occurs. This criterion can also be applied in the case of fractures occurring inside the specimen. In this paper is presented how stress based formability diagram can be determined based on data obtained from the strain-based formability diagram.
- Stress-based formability diagram is more important since its shows a significant impact of stress state on the magnitude of the limit strain (Figure 4).
- This study showed that strain-based formability diagram can be transformed into a stress-based one.
- The reverse transformation of stress-based formability diagram into a strain-based formability diagram is also possible, as demonstrated in [19].
- The application of FLD enables the prediction of limit strain in real forming processes and the optimization of the number of stages.
- Results of multi stage upsetting of prismatic specimen by V shape die proves the existance of a small reserve of material formability after 17 stages.

Note:
This paper is based on the paper presented at COMETa 2018 – The 4th International Conference on Mechanical Engineering Technologies and Applications, organized by Faculty of Mechanical Engineering, University of East Sarajevo, in Jahorina, BOSNIA & HERZEGOVINA, between 27–30 November, 2018.

REFERENCES

[1] P. Gänser, (2001), "Free-surface ductility in bulk forming processes", International Journal of Plasticity, Vol. 17, pp. 755-772.
[2] A. R. Ragab, (2002),"Fracture limit curve in upset forging of cylinders", Materials Science and Engineering: A, Vol.334, pp. 114-119.
[3] J. Landre, A. Pertence, P. R. Cetlin, J. M. C. Rodrigues, P. A. F. Martins, (2003), "On the utilization of ductile fracture criteria in cold forging", Finite Elements in Analysis and Design, Vol.39, pp. 175-186.
[4] G. Dieter, H. Kuhn, L. Semiatin,(2003),"Handbook of Formability and Process Design",Chapter 2 Bulk Formability of Metals, Chapter 3 Evolution of Microstructure during Hot Working, ASM International, Material Park Ohio.
[5] V. Vujovic, A. Shabaik, (1986), "Formability Criteria for Ductile Fracture", Trans. ASME J. Engng. Mater. Technol., Vol. 108, pp. 245-249.
[6] D. Vilotic, M. Plancak, Đ. Čupković, S. Alexandrov, N. Alexandrov, (2006), "Free Surface Fracture in Three Upsetting Tests", Experimental Mechanics, Vol. 46, pp. 115-120.
[7] D. Vilotić, S. Alexandrov, M. Plančak, D. Movrin, A. Ivanišević, M. Vilotić, (2011), "Material Formability at Up-setting by V–Shape Dies", Steel Research International, Special Edition, pp. 923-928.
[8] D. Vilotic, N. Chikanova, S. Alexandrov, (1999), "Disk Upsetting Between Spherical Dies and its Application to the Determination of Forming Limit Curves", Journal Strain Analysis, Vol. 34, pp. 17-22.
[9] S. Alexandrov, N. Chikanova, D. Vilotic, (1997), "Compression of a Block Between Cylindrical Dies and its Application to the Formability Diagram", Studies in Applied Mechanics, Advanced Methods in Materials Processing Defects, Vol. 45, pp. 247-256.

[10] D. Vilotic, N. Chikanova, S. Alexandrov, (1999), "Disk Upsetting Between Spherical Dies and its Application to the Determination of Forming Limit Curves", Journal Strain Analysis, Vol.34, pp. 17-22.
[11] D. Vilotic, M. Plancak, S. Grbic, S. Alexandrov, N. Chikanova, (2001), "An approach to determining the formability diagram based on upsetting tests", Fatigue Fract. Engng. Mater. Struct., Vol 26, pp. 305-310.
[12] S. Alexandrov, D. Vilotic, Z. Konjovic, M. Vilotic, "An Improved Method for Determining the Formability Diagram", Experimental Mechanics, 2013, Vol 53, pp.699-711.
[13] D. Vilotic, S. Alexandrov, M. Plancak, M. Vilotic, A. Ivanisevic, I. Kacmarcik,(2012), "Material Formability at Upsetting by Cylindrical and Flat Dies", Steel Research International, special issue, pp 1175-1178.
[14] V. L. Kolmogorov, (2001), "Mehanika obrabotki metallov davleniem", UPI, Ekaterinburg.
[15] D. Vilotić (1987), "Ponašanje čeličnih materijala u obradnim sistemima hladnog zapreminskog deformisanja", Univerzitet u Novom Sadu, Fakultet tehničkih nauka.
[16] D.Breuer, (2007), "Bestimmung des Formänderungsvermögens bei der Kaltmassivumformung", Berichte aus der Produktionstechink, band 19, Sharker Verlag.
[17] S. Alexandrov, D. Vilotic, R. Goldstein, N. Chikanova, (1999), "The Determination of the Formability Diagram", Mechanics of Solids, Vol 34, pp. 118-125.
[18] D. Vilotic, S. Alexandrov, M. Plancak, A. Ivanisevic, (2012), "Use of Non-Axisymmetric Specimens in Upsetting for Determining the Formability Diagram", Proceeding of 19. European Conference on Fracture - ECF, Kazan: EuropeanStructural Integrity Society, ISBN 978-5-905576-18
[19] D. Vilotić, S. Alexandrov, A. Ivanišević, M. Milutinović, (2016), "Reducibility of Stress-Based Formability Diagram to Strain-Based Formability Diagram", International Journal of Applied Mechanics, Vol. 8, No. 02, (doi: 10.1142/S1758825116500228)
[20] M. Vilotić, (2015), "Intenzivna plastična deformacija u procesima višefaznog sabijanja materijala", doktorska disertacija, Univerzitet u Novom Sadu, Fakultet tehničkih nauka.

ACTA TECHNICA CORVINIENSIS BULLETIN OF ENGINEERING
ISSN: 2067-3809